

A model for nonlinear hysteretic and ratcheting behaviour

Houlsby, G.T.¹, Abadie, C.N., Beuckelaers, W.J.A.P. and Byrne, B.W.

Department of Engineering Science, University of Oxford
Parks Road, Oxford OX1 3PJ, UK

Abstract

We present a theoretical model to describe the response of a one dimensional mechanical system under cyclic loading. Specifically, the model addresses the non-linear response on loading, hysteretic behaviour on unloading and reloading, and the phenomenon of ratcheting under very many cycles. The methods developed are formulated within the hyperplasticity framework. The model can be expressed in the form of general incremental relationships, can therefore be applied without modification directly to any loading history, and can be readily implemented within a time-stepping numerical code. A rigorous procedure is described to accelerate the ratcheting process, so that the effects of very large numbers of cycles can be analysed through a reduced number of cycles. A generalisation from unidirectional to multidirectional loading is described, together with a tensorial form for application to material modelling. The original motivation was for the application to design of piles under lateral loading, and an example of this application is provided. However, the model is equally applicable to many other problems involving unidirectional or bi-directional cyclic loading in which the system exhibits a similar character of hysteretic behaviour, with ratcheting under large numbers of cycles.

Keywords: cycling, hysteresis, plasticity, ratcheting

1. Introduction

There are numerous problems in engineering in which the response at small strain (or displacement) is readily characterised as elastic; at larger strains a nonlinear response is observed; and unloading-reloading cycles exhibit hysteretic behaviour. The hysteresis often conforms closely to the “Masing rules” (Masing, 1926). This type of response can be described theoretically by multi-surface plasticity models with kinematic hardening. However, when very large numbers of cycles are applied, many such problems exhibit ratcheting (accumulation of strain or deformation). Our purpose here is to develop a modelling framework capable of capturing this ratcheting response.

The initial motivation for this model development came from the analysis of “monopile” foundations for offshore wind turbines under lateral loading. This is a problem in which many cycles of different amplitude are applied during the lifetime of the structure, and because of a bias in loading due to the predominant wind direction, ratcheting is a potential problem. We are concerned

¹ Corresponding author: guy.houlsby@eng.ox.ac.uk

with the macroscopic response, which can be expressed in terms of the relationship between applied load H and the corresponding displacement u , see Figure 1. Such a “macro-element” approach proves to be extremely useful in efficiently representing the piled foundation behaviour within structural analyses, without the need to model details of the distribution of loads along the pile. The “macro-element” approach, which can be regarded as a special case of sub-structuring, is widely used in geotechnical engineering for applications to soil-structure interaction. It permits the entire response of the soil/foundation system to be encapsulated in a single model, greatly simplifying analyses and allowing an efficient link to structural analysis. Macro-models were pioneered by Schotman (1989) and Nova and Montrasio (1991). Well established models for shallow foundations on clay and sand are reported by Martin and Houlsby (2001) and by Houlsby and Cassidy (2002). Such models are of particular importance in the offshore industry, where they have become a standard method of analysis. More recently they have also been applied to deep foundations (piles), see for example Gerolymos *et al.* (2014)

Our goal here is to develop a realistic model for a pile under working conditions, so that this can be implemented in numerical analyses of a turbine under fatigue loading. We therefore place most emphasis on working loads and large numbers of cycles, and are less concerned here with modelling of the pile capacity under extreme loading.

For very small loads it may be sufficient to describe the response as linear, but as soon as loads become a significant fraction of the ultimate capacity (say more than 10% to 20%), the response becomes non-linear (shown schematically as AB in Figure 2). On unloading, a stiff response (BC in Figure 2) is observed, but this too becomes slightly non-linear for significant load reversals. The result is that during an unload-reload cycle (BCD in Figure 2) a hysteresis loop is observed, resulting in dissipation of energy during the cycle. However, if several similar one-way cycles are applied, it is noted that the hysteresis loop does not exactly close (point D is separate from point B), so that after many cycles an accumulated “ratcheting” displacement develops (EFG in Figure 2). This is true of any cycling other than symmetric 2-way cycling. However, the rate of accumulation of ratcheting displacement gradually reduces as the number of cycles increases (compare EFG to HIJ in Figure 2 with BCD to EFG). Also, it is observed that the shapes of the hysteresis loops change, with less hysteresis (less dissipation) after many cycles (compare BCD, EFG and HIJ in Figure 2).

All of these features are illustrated in Figure 3, showing one of the model tests reported by Abadie (2015). These observed features of pile behaviour were also reported by LeBlanc, Houlsby and Byrne (2010), who developed empirical expressions for fitting the (relatively small) changes in secant stiffness of cycles and the (more significant) accumulation of “ratcheting” strain during very many cycles. Their empirical fitting of the data was extended by LeBlanc, Byrne and Houlsby (2010), who suggested a way by which multi-amplitude cycling could be accommodated within the empirical framework. Further relevant experimental results are reported by Abadie (2015). Our purpose here is to move on from such purely empirical approaches to develop an incremental model that is capable of capturing this type of response.

Although the above problem provides the motivation for this work, the model itself has much wider applicability. We return to the piling problem in an example at the end of this paper, but the main

development is in more general terms, and is therefore expressed in terms of “stress and “strain”. The model could be applied to any one-dimensional problem in which the mechanical response shows similar overall features to those illustrated in Figures 2 and 3. We also describe a logical extension of the model to two dimensional problems, which is straightforward. Of course the “macro model” simply represents in a compact way the integrated response of the pile-soil foundation system. At the next level of detail, this is often modelled by the so-called “ p - y ” (generalised Winkler) approach, in which the lateral load at any point on the pile (p) is expressed as a function of the local displacement (y). The approach we describe here can be implemented as a “ p - y ” model, as shown by Beuckelaers *et al.* (2016). Taking this one step further, we expect that the macro model reflects features of the underlying constitutive response of the soil itself. In principle therefore we expect that the same modelling approach could be extended to encompass a full tensorial constitutive model of material behaviour, but whilst we provide a brief outline of one such model, we do not underestimate the complexity of calibrating such a model against real data.

Brief review of existing approaches to ratcheting

Almost all models currently used to describe ratcheting behaviour (principally with application to modelling alloys) can be traced back to the Armstrong-Frederick (AF) model, with many variants being published. A useful review is provided by Chaboche (2008) and some of the key developments are described below. The AF approach was originally published in a CEGB report, Armstrong and Frederick (1966), not available in the open literature until reprinted as Frederick and Armstrong (2007). It was proposed as a means of describing the Bauschinger effect in a model that employed just a single, kinematically hardening von Mises type yield surface. A particular incremental form was proposed for the evolution law for the back-stress. The method introduced a *recovery term* that describes an evanescent memory of the loading history, making the kinematic hardening non-linear. An apparently unwanted side effect of the form of the evolution law was that asymmetric cycling resulted in accumulation of strain in the direction of the applied stress, *i.e.* ratcheting. Nowadays the Bauschinger effect (and other effects of stress history) would normally be captured by adopting multiple-surface kinematically hardening models, which naturally result in cyclic behaviour which accords with the Masing rules. Ironically therefore, the original purpose of the AF model is superseded, whilst the unwanted by-product of ratcheting has formed the basis of almost the entire literature on ratcheting.

Although the AF model results in the accumulation of plastic strain at each cycle, the increment of ratcheting strain is constant for similar cycles. The accumulated ratcheting strain is usually therefore over-predicted (Ohno and Wang, 1995, Lemaitre and Chaboche, 2010) and the initial cyclic load response does not conform to the Masing rules. Chaboche (1986) and Chaboche and Nouailhas (1989) proposed a method to accommodate a varying rate of ratcheting by superimposing a small number of AF surfaces, with 2 to 5 surfaces usually used in practice (*e.g.* 3 surfaces in the commercial code ABAQUS). If one of the surfaces just involves conventional linear hardening then ratcheting at a decreasing rate can be captured (Lemaitre and Chaboche, 2010). However, in this case, the model usually exhibits a stabilising asymptotic response where ratcheting stops (Lemaitre and Chaboche, 2010) and the transient accumulated ratcheting strain is often over-predicted (Bari and Hassan, 2000, Lemaitre and Chaboche, 2010).

A considerable amount of research has been carried out on this family of models (*e.g.* Ohno and Wang, 1995, Chaboche, 1991). Nevertheless, the determination of the model parameters requires an extensive data base including tensile curves, cyclic curves, stabilised strain-stress loops and ratcheting tests with increasing mean load (Chaboche, 1991). Since the micro- and meso-phenomena in alloys and soils are very different, the applicability of the AF approach directly to geotechnical problems is questionable, especially with regard to parameter identification.

The AF model is derived in the terminology of hyperplasticity in Appendix C, in order to facilitate comparison of our approach with what is the *de facto* standard approach to modelling of ratcheting. Comparison of Figures 8 and 13 (discussed in detail later), and the associated energy, dissipation and constraint expressions, shows that the two approaches are conceptually very similar, with the key difference being that the ratcheting element in the AF model is in series with just the spring element of a spring-slider combination, whilst in our approach it is placed in series with the combined element. This change has the important consequence (for the series version of our model) that when the model is extended to multiple yield surfaces only a single ratcheting element needs to be introduced (see Figure 8) rather than a separate one associated with each spring, as would be implied by the AF model. This difference results in considerable simplification of the model, and the calibration of the necessary parameters. The parallel version of our model (Figure 9) is less easily compared with AF.

Purpose of this paper

Our purpose here is to present a theoretical framework (HARM - “Hyperplastic Accelerated Ratcheting Model”) that captures all of the phenomena observed in Figures 2 and 3. The model is formulated using the hyperplasticity approach (Houlsby and Puzrin, 2006), which offers the following advantages: (a) it guarantees that the model is consistent with the Laws of Thermodynamics, (b) the entire definition of the model is achieved through the specification of just two scalar functions, with the incremental response being derived by application of standardised procedures, and therefore (c) the model is mathematically concise and consistent.

In order to emphasise this generality of the model, we develop the model using the terminology of “stress” and “strain” (σ, ϵ). In the particular application to lateral loading of piles, Figure 1, the “stress” would stand for the lateral load on the pile H and the “strain” for the displacement at the point of load application u . Of course, for this and other applications, careful attention needs to be applied to the appropriate dimensions for all quantities, and in particular for the stiffness. The stress and strain must form a work-conjugate pair.

For a pile in a cross-anisotropic soil (*i.e.* with the same properties in all horizontal directions) the response to loading in any direction should be the same, and this would be true of many two-dimensional loading problems possessing a similar symmetry. For these cases we develop a generalisation of the HARM model to two dimensions, although we do not yet have experimental data to support this generalisation.

In the following we set out the overall structure of a model which captures the features observed empirically as described above. This general model employs a number of functions which can be

chosen to fit empirical data. The calibration of these empirical functions against a particular set of model pile tests in sand is the subject of Abadie *et al.* (2016), and is also described in detail by Abadie (2015).

2. Theoretical background

This paper employs the “hyperplasticity” framework for describing the non-linear behaviour of materials which is presented by Houlsby and Puzrin (2006). This approach goes back to the original work by Ziegler (1963), later described in more detail by Ziegler (1977). Although not at that time termed hyperplasticity, the complete formulation as applied to plastic (rate-independent) materials was set out by Houlsby (1981). Later developments, including extensive use of Legendre Transforms to reformulate the models, were described by Collins and Houlsby (1997), Houlsby and Puzrin (2000), and the entire approach summarised by Houlsby and Puzrin (2006). The approach has much in common with the “standard material” approach set out by Germain *et al.* (1983), which in turn draws heavily on Suquet (1982), and has roots in the work of Moreau (1970). In particular Germain *et al.* (1983) draw the conclusion “*all the constitutive equations of the material can be recast in two non-negative closed functions*” that is central to hyperplasticity.

The hyperplasticity method focuses on the use of internal variables (in this application interpreted as plastic strains) to describe the history of loading. A single internal variable (plastic strain) can capture basic elastic-plastic behaviour, but to describe the response under more complex loading histories, multiple internal variables can be used. This process can be taken to its logical conclusion in which an infinite number of internal variables (*i.e.* an internal function) is used to describe the loading history, Puzrin and Houlsby (2001a). However, for numerical implementation, a finite number of variables must be employed, so here we employ the formulation using a finite number of internal variables, following closely the development of kinematic hardening models in Puzrin and Houlsby (2001b), but with the addition of ratcheting. With a sufficient number of internal variables, continuous curves may be approximated with any desired level of accuracy.

The hyperplasticity framework is applicable to rate-independent or rate-dependent materials. However, even if the material itself is rate-independent, there are certain advantages in formulating the model as the limiting case of a rate-dependent material, with an artificial (very small) “viscosity”. We include details of such an approach here, following Houlsby and Puzrin (2002), as this allows a particularly straightforward numerical implementation.

Finally, there is a choice available of the scalar functions used to define a particular model. Thus the stored energy may be defined in terms of the Helmholtz free energy (with strain as the independent variable) or the Gibbs free energy (with stress as the independent variable). These functions are not independent, but are related through a Legendre Transform, so specification of just one of them is sufficient. We present the principal results here in terms of the Helmholtz free energy, but also include expressions for the Gibbs free energy in Appendix B.

For the rate-independent formulation, the dissipative response can be expressed through the dissipation function (with rate of internal variable as the independent variable) or specification of a

yield surface (with generalised stress as the independent variable). We present the model first in terms of the dissipation function, but also quote the form of the yield function. Similarly, for the rate-dependent formulation, the dissipative response can be expressed through the force potential (with rate of internal variable as the independent variable) or the flow potential (with generalised stress as the independent variable). In this case, because it is better suited to numerical implementation, we concentrate here on use of the flow potential.

A succinct presentation of the fundamental equations for the formulation is given in Appendix A; for more detail, see Houlsby and Puzrin (2006).

3. Basic kinematic hardening models

Conceptual framework

The starting point for this development is a multisurface plasticity model using pure kinematic hardening, as described by Puzrin and Houlsby (2001b) and illustrated conceptually in Figure 4. The model consists of an elastic element in series with a number of elements, each consisting of a spring and slider element in parallel. The strengths of the sliding elements range from the stress at which first yield occurs to the ultimate strength that is to be modelled. The spring elements in parallel with each slider provide pure kinematic hardening, with the result that the stress-strain response is multilinear, as illustrated in Figure 5(a). For a sufficiently large number of sliding elements a smooth curve, Figure 5(b), can be approximated with adequate accuracy. On unloading and reloading hysteresis occurs according to the “Masing rules” (which arise as a consequence of the mechanics of the model, and are not implemented as separate assumptions), Masing (1926). These result in hysteretic behaviour, Figure 5(c). This model can therefore capture all the phenomena described above except for ratcheting. The new model developed later in this paper includes the modifications that allow ratcheting to be captured too.

Mathematical formulation of the series form

The model is expressed in terms of conjugate stress and strain variables σ, ε . The model employs internal variables α_n , $n=1..N_s$, each conjugate to a generalised stress $\chi_n = \bar{\chi}_n$ (see Houlsby and Puzrin, 2006), and which play the role of plastic strain components. The total plastic strain is given

$$\text{by } \varepsilon_p = \sum_{n=1}^{N_s} \alpha_n .$$

In terms of the parameters defined on Figure 4, the model is fully described by the Helmholtz free energy:

$$f = \frac{H_0}{2} \left(\varepsilon - \sum_{n=1}^{N_s} \alpha_n \right)^2 + \sum_{n=1}^{N_s} \frac{H_n}{2} \alpha_n^2 \quad \dots(1)$$

and dissipation function:

$$d = \sum_{n=1}^{N_S} k_n |\dot{\alpha}_n| \quad \dots(2)$$

The full development of such a model is explored by Houlsby and Puzrin (2003a), and we do not repeat the derivation here as it is a simpler form of the development in Section 4 below. The break points in the stress-strain curves and the tangent moduli (see Figure 6) are defined by:

$$\sigma_n = k_n, \quad n = 1 \dots N_S \quad \dots(3)$$

$$\varepsilon_n = \sum_{i=0}^{n-1} \frac{k_n - k_i}{H_i}, \quad n = 1 \dots N_S, \text{ defining } k_0 = 0 \quad \dots(4)$$

$$\frac{1}{E_n} = \sum_{i=0}^n \frac{1}{H_i}, \quad n = 0 \dots N_S \quad \dots(5)$$

Given a primary loading curve, the above expressions allow the parameters N_S, k_n, H_n to be chosen to fit the curve to any desired level of accuracy (see Abadie *et al.*, 2016).

Parallel form

An equivalent model can be formulated in which the spring/slider elements act in parallel, as illustrated in Figure 7. This model too results in the Masing Rules for unload-reload behaviour. With appropriate calibration of the constants, the series and parallel models (Figures 4 and 7) are therefore indistinguishable in the one-dimensional case. However, they do give rise to subtle differences in response when generalised to two dimensions. As we know of no experimental data that would distinguish between these alternatives, we pursue both options here. The parallel model is defined by:

$$f = \sum_{n=1}^{N_S} \frac{H_n}{2} (\varepsilon - \alpha_n)^2 + \frac{H_{N_S+1}}{2} \varepsilon^2 \quad \dots(6)$$

$$d = \sum_{n=1}^{N_S} k_n |\dot{\alpha}_n| \quad \dots(7)$$

The break points in the stress-strain curves and the tangent moduli (see Figure 6) are defined by:

$$\sigma_n = \sum_{i=1}^n k_i + \sum_{i=n+1}^{N_S+1} H_i \varepsilon_n = \sum_{i=1}^n k_i + \frac{k_n}{H_n} \sum_{i=n+1}^{N_S+1} H_i, \quad n = 1 \dots N_S \quad \dots(8)$$

$$\varepsilon_n = \frac{k_n}{H_n}, \quad n = 1 \dots N_S \quad \dots(9)$$

$$E_n = \sum_{i=n+1}^{N_S+1} H_i, \quad n=0 \dots N_S \quad \dots(10)$$

4. Extension to ratcheting models

The incorporation of ratcheting into plasticity models in a consistent manner is a surprisingly intractable problem, and most simple variants of the above multiple surface models simply exhibit closed cycles (plastic accommodation) without ratcheting. The concept behind the ratcheting models developed here is that, in addition to the plastic strains already defined, there is an additional “ratcheting strain” α_r which can be understood as follows, and is illustrated schematically in Figure 8. Whenever plastic strains occur, an additional “ratcheting strain” occurs which is a small fraction R of the plastic strain (R is a positive variable). However, irrespective of the direction of the plastic strain, the ratcheting strain always occurs in the direction of the applied stress. In the following we allow for a different ratio R_n to be associated with each plastic strain

variable α_n , defining the ratcheting strain as $\dot{\alpha}_r = S(\sigma) \sum_{n=1}^{N_S} R_n |\dot{\alpha}_n|$, where $S(\dots)$ is a modified signum

function (see Notation). In order to calibrate the model against data, the value of R_n may be a function of a number of variables (see later discussion), and in particular it may be a function of the magnitude of the current stress.

Series form

The “series” version of the HARM model, s-HARM, illustrated in Figure 8 is completely defined (in its rate-dependent form) by the two scalar functions:

$$f = \frac{H_0}{2} \left(\varepsilon - \sum_{n=1}^{N_S} \alpha_n - \alpha_r \right)^2 + \sum_{n=1}^{N_S} \frac{H_n}{2} \alpha_n^2 \quad \dots(11)$$

$$d = \left(\sum_{n=1}^{N_S} k_n |\dot{\alpha}_n| \right) + \sigma \dot{\alpha}_r \quad \dots(12)$$

Together with a constraint which defines the ratcheting strain

$$c = \dot{\alpha}_r - S(\sigma) \sum_{n=1}^{N_S} R_n |\dot{\alpha}_n| = 0 \quad \dots(13)$$

These equations can be seen to be developments of equations (1) and (2).

The reasons for the choice of these functions may not be immediately apparent to a reader unfamiliar with the hyperplasticity approach, but the following derivations demonstrate how these functions, with appropriate choice of parameters, give rise to a model with the features that are desired.

Following Appendix A, and first forming $d^* = d + \Lambda c$, where Λ is a Lagrangian multiplier, the complete description of the model is achieved through the derivations:

$$\sigma = \frac{\partial f}{\partial \varepsilon} = H_0 \left(\varepsilon - \sum_{n=1}^{N_S} \alpha_n - \alpha_r \right) \quad \dots(14)$$

$$\bar{\chi}_n = -\frac{\partial f}{\partial \alpha_n} = H_0 \left(\varepsilon - \sum_{n=1}^{N_S} \alpha_n - \alpha_r \right) - H_n \alpha_n = \sigma - H_n \alpha_n, \quad n=1 \dots N_S \quad \dots(15)$$

$$\bar{\chi}_r = -\frac{\partial f}{\partial \alpha_r} = E \left(\varepsilon - \sum_{n=1}^{N_S} \alpha_n - \alpha_r \right) = \sigma \quad \dots(16)$$

$$\chi_n = \frac{\partial d^*}{\partial \dot{\alpha}_n} = k_n S(\dot{\alpha}_n) - \Lambda S(\sigma) R_n S(\dot{\alpha}_n), \quad n=1 \dots N_S \quad \dots(17)$$

$$\chi_r = \frac{\partial d^*}{\partial \dot{\alpha}_r} = \sigma + \Lambda \quad \dots(18)$$

From the above we can derive $\Lambda = 0$ and:

$$\sigma = H_0 \left(\varepsilon - \sum_{n=1}^{N_S} \alpha_n - \alpha_r \right) \quad \dots(19)$$

$$\sigma = k_n S(\dot{\alpha}_n) + H_n \alpha_n, \quad n=1 \dots N_S \quad \dots(20)$$

For numerical implementation the response is required incremental form. Differentiation of (19) gives:

$$d\sigma = H_0 \left(d\varepsilon - \sum_{n=1}^{N_S} d\alpha_n - d\alpha_r \right) \quad \dots(21)$$

From (20) we derive that if $|\sigma - H_n \alpha_n| < k_n$, i.e. yielding does not occur, $d\alpha_n = 0$. If $|\sigma - H_n \alpha_n| = k_n$ then yielding can occur, $d\alpha_n \neq 0$ with $d\sigma = H_n d\alpha_n$ (the consistency condition). Together with

$d\alpha_r = S(\sigma) \sum_{n=1}^{N_S} R_n |d\alpha_n|$ (from the constraint equation) these relationships define fully the

incremental elastic-plastic behaviour.

Parallel form

The alternative version of the model (p-HARM) arranges the spring-slider units in parallel rather than in series, see Figure 9. This model would be described through the functions:

$$f = \sum_{n=1}^{N_S} \frac{H_n}{2} (\varepsilon - \alpha_n - \alpha_r)^2 + \frac{H_{N_S+1}}{2} (\varepsilon - \alpha_r)^2 \quad \dots(22)$$

$$d = \left(\sum_{n=1}^{N_S} k_n |\dot{\alpha}_n| \right) + \sigma \dot{\alpha}_r \quad \dots(23)$$

$$c = \dot{\alpha}_r - S(\sigma) \sum_{n=1}^{N_S} R_n |\dot{\alpha}_n| = 0 \quad \dots(24)$$

Note that equations (22) and (23) are the same as (12) and (13), although the physical interpretation of the variables and parameters in the p-HARM model differs from that in s-HARM. The development follows exactly the same process as in equations (14) to (18), with the end result that (19) and (20) are replaced by:

$$\sigma = \sum_{n=1}^{N_S} H_n (\varepsilon - \alpha_n - \alpha_r) + H_{N_S+1} (\varepsilon - \alpha_r) \quad \dots(25)$$

$$H_n (\varepsilon - \alpha_n - \alpha_r) = k_n S(\dot{\alpha}_n), \quad n = 1 \dots N_S \quad \dots(26)$$

Alternative derivations of s-HARM and p-HARM, including rate-dependent forms that lead in particularly simple ways to the full incremental relationships, are given in Appendix B, sections B3 and B4.

5. Variable ratcheting rate

Whilst the above models are capable of modelling ratcheting, they have the property that a series of identical cycles each produces an identical amount of ratcheting strain. In practice it is desired to include one or more of the three features noted above: with an increasing number of cycles there is (a) a reduction of ratcheting rate, (b) a reduction in dissipated energy per cycle (*i.e.* tightening of the hysteresis loop) and (c) an increase in secant stiffness.

These effects can be taken into account by changing the parameters that govern the ratcheting rate as ratcheting progresses. The most straightforward means of achieving this is to introduce a scalar hardening parameter β to the model, defined in such a way that it increases monotonically with plastic dissipation or cyclic loading history. Some possible choices for the evolution of β are, for

instance, $\dot{\beta} = d$, $\dot{\beta} = \sum_{n=1}^{N_S} k_n |\dot{\alpha}_n|$, $\dot{\beta} = \sum_{n=1}^{N_S} |\dot{\alpha}_n|$, $\dot{\beta} = \sigma \dot{\alpha}_r$ or $\dot{\beta} = |\dot{\alpha}_r|$. We leave open at this stage the

choice of the evolution equation for β , which is simply introduced into the formulation as a passive internal variable as detailed in Appendix A, section A5. No changes are necessary to the defining equations for the models, other than to include also the relevant evolution equation for β . However, by making certain quantities (specifically k_n and R_n) functions of β , it is possible to capture the above desired effects, as illustrated in the model described below. Note, however, that

if the parameters that appear in the free energy expression (equations 11 or 22) are made functions of β , then additional terms appear in the differentials: in practice this applies only if the stiffness parameters H_n are functions of β .

As it is based on expressions for the storage and dissipation of energy, the thermodynamic approach invites a physical interpretation of the particular chosen functions. In principle they represent respectively the integration of the storage and dissipation in the entire continuum represented by the macro model. If the relevant expressions were established at a microscopic scale then it might be possible to infer the macro model from these, but unfortunately this problem is intractable. We can, however, make some observations. The stored energy will include components coming both from the elastic deformation of the pile, and from the deformation of the soil, whilst the dissipation will arise (almost) entirely in the soil. For a relatively stiff pile the contribution of the pile to the stored energy will be small, so the entire response will be dominated by the soil behaviour. The behaviour of the soil is in turn dominated by the response at particle-to-particle contacts, which undergo elastic deformation and slip. The modelling of this behaviour by a large number of elastic-plastic sliding elements (with the attendant stored and dissipative terms) mimics at the macro scale the microscopic mechanisms that occur.

The novelty in the ratcheting model lies obviously in the additional ratcheting element which is linked to the plastic deformation through the constraint expression. Only minor adjustments are made to the dissipation, and none to the stored energy. The concept that is represented is that the sliding processes are imperfect: the sliding in one direction may involve very slightly different processes than sliding in the other, resulting in a residual deformation. Furthermore, these processes are heavily biased by the applied stress (as expressed in equations 13, 24 and 40). The reduction in rate of ratcheting though a hardening process is an empirical observation which may be explained by gradual rearrangement of the granular structure to accommodate better the applied loads.

6. Accelerated modelling

One of the problems with the modelling of high-cycle fatigue or ratcheting problems is that it becomes impracticable to model every cycle individually: computation times for thousands or even millions of cycles are prohibitive. The cumulative effects of cycling are therefore accounted for by a variety of empirical procedures, see for example LeBlanc, Byrne and Houlsby (2010) for the example of loading of a monopile. Whilst these can be applied to problems for relatively simple loading histories, they are difficult to implement within numerical codes, and are of questionable applicability for more complex load paths, for instance multi-amplitude or pseudo-random cyclic events.

An advantage of the method described above is that it can be adapted to accelerate the effects of accumulated deformations by the simple expedient of multiplying the ratcheting parameters R_n in equations (13) or (23) by an additional factor R_{fac} :

$$\dot{\alpha}_r = R_{fac} S(\sigma) \sum_{n=1}^N R_n |\dot{\alpha}_n| \quad \dots(27)$$

At the same time, if the evolution equation for β employs a measure that is essentially dependent on the plastic strain rather than ratcheting strain, then the evolution equation also needs to be modified to account for the reduced plastic strain in the reduced number of cycles, for instance this

would require $\dot{\beta} = R_{fac} \sum_{n=1}^{N_s} k_n |\dot{\alpha}_n|$ or $\dot{\beta} = R_{fac} \sum_{n=1}^{N_s} |\dot{\alpha}_n|$, whilst $\dot{\beta} = \sigma \dot{\alpha}_r$ or $\dot{\beta} = |\dot{\alpha}_r|$ would remain

unchanged. These changes represent purely a numerical artifice to increase the rate of accumulation of ratcheting strain in the analysis, and do not change the underlying model (for instance, compare Figures 11 and 12 in the example discussed in Section 9).

It can be shown that the acceleration process is exact if the shape of the underlying unload-reload loop (excluding the ratcheting terms) is not modified as ratcheting proceeds. If, however, this is not the case (for example if the k_n or H_n are functions of β) and the loop does change as ratcheting progresses, then the acceleration method is approximate only. It can nevertheless still be valuable, as provided that any changes in the loop shape are small in any one (accelerated) cycle, it can provide a good approximation to the exact result.

7. Two-dimensional models

With a self-evident notation, an equivalent two-dimensional s-HARM model, which could be used to model multi-axial loading, can be defined by:

$$f = \frac{H_0}{2} \left[\left(\varepsilon_1 - \sum_{n=1}^{N_s} \alpha_{1n} - \alpha_{1r} \right)^2 + \left(\varepsilon_2 - \sum_{n=1}^{N_s} \alpha_{2n} - \alpha_{2r} \right)^2 \right] + \sum_{n=1}^{N_s} \frac{H_n}{2} (\alpha_{1n}^2 + \alpha_{2n}^2) \quad \dots(28)$$

$$d = \left(\sum_{n=1}^{N_s} k_n \sqrt{\dot{\alpha}_{1n}^2 + \dot{\alpha}_{2n}^2} \right) + \sigma_1 \dot{\alpha}_{1r} + \sigma_2 \dot{\alpha}_{2r} \quad \dots(29)$$

$$c_i = \dot{\alpha}_{ir} - S_i(\sigma) \sum_{n=1}^{N_s} R_n \sqrt{\dot{\alpha}_{1n}^2 + \dot{\alpha}_{2n}^2} = 0 \quad \dots(30)$$

where the vectorial generalized signum function $S_i(\)$ is as defined in the Notation.

It can readily be confirmed that for either $\sigma_1 = 0$ or $\sigma_2 = 0$ this reduces to the one-dimensional case, and further it can be shown that the two-dimensional model is isotropic: the unidirectional response is the same irrespective of loading direction. The model is thus a satisfactory generalization to the two-dimensional case, although the accuracy of the generalization would need to be determined by experiment. Note that no additional parameters are required for the two-

dimensional model. In a similar way the two-dimensional version of the p-HARM model is specified through replacing equation (22) by:

$$f = \sum_{n=1}^{N_s} \frac{H_n}{2} \left((\varepsilon - \alpha_{1n} - \alpha_{1r})^2 + (\varepsilon - \alpha_{2n} - \alpha_{2r})^2 \right) + \frac{H_{N_s+1}}{2} \left[(\varepsilon_1 - \alpha_{1r})^2 + (\varepsilon_2 - \alpha_{2r})^2 \right] \quad \dots(31)$$

In the two dimensional models the hardening parameter is again required to be a monotonically increasing scalar, for instance the equivalent to the example given later in Section 9 would be

$$\dot{\beta} = \sum_{n=1}^{N_s} \sqrt{\dot{\alpha}_{1n}^2 + \dot{\alpha}_{2n}^2}.$$

The above generalisations also provide a basis for generalisation of our approach to multiaxial loading in more than two dimensions.

8. Tensorial models

In principle the HARM approach could be applied to a wide variety of plasticity-based continuum models to include the effects of ratcheting. Here we develop just one such model, based on a multi-surface kinematic hardening model with a series of von Mises type yield surfaces, Puzrin and Houlsby (2001b). The underlying model would be defined in its series form (without ratcheting) by the functions:

$$f = \frac{K}{2} \varepsilon_{ij} \varepsilon_{ij} + G \left(\varepsilon'_{ij} - \sum_{n=1}^N \alpha'_{ij}{}^n \right) \left(\varepsilon'_{ij} - \sum_{n=1}^N \alpha'_{ij}{}^n \right) + \sum_{n=1}^N H_n \alpha'_{ij}{}^n \alpha'_{ij}{}^n \quad \dots(32)$$

$$d = \sum_{n=1}^N k_n \sqrt{2} \sqrt{\dot{\alpha}'_{ij}{}^n \dot{\alpha}'_{ij}{}^n} \quad \dots(33)$$

together with the plastic incompressibility constraint $c_n = \dot{\alpha}'_{kk}{}^n = 0$.

This could be extended to the ratcheting model by modifying the functions to:

$$f = \frac{K}{2} \varepsilon_{ij} \varepsilon_{ij} + G \left(\varepsilon'_{ij} - \sum_{n=1}^N \alpha'_{ij}{}^n - \alpha'_{ij}{}^r \right) \left(\varepsilon'_{ij} - \sum_{n=1}^N \alpha'_{ij}{}^n - \alpha'_{ij}{}^r \right) + \sum_{n=1}^N H_n \alpha'_{ij}{}^n \alpha'_{ij}{}^n \quad \dots(34)$$

$$d = \sum_{n=1}^N k_n \sqrt{2} \sqrt{\dot{\alpha}'_{ij}{}^n \dot{\alpha}'_{ij}{}^n} + \sigma_{ij} \dot{\alpha}'_{ij}{}^r \quad \dots(35)$$

and the constraint that defines the ratcheting rate:

$$c_r = \dot{\alpha}'_{ij}{}^r - S_{ij}(\sigma') \sum_{n=1}^N R_n \sqrt{\dot{\alpha}'_{ij}{}^n \dot{\alpha}'_{ij}{}^n} = 0 \quad \dots(36)$$

9. Example calculation

We now illustrate the above method by defining one particular realisation of the s-HARM series model. This involves choices of functions that are found empirically to match well the behaviour of a model monopile tested in sand, Figure 1. In the specific case of modelling pile response the variables (σ, ε) stand for (H, u) . We use this example for illustration only: the specific forms of the fitting equations have been chosen for convenience, and are not fundamental to the underlying model. We acknowledge that the real behaviour of laterally loaded piles may be complicated by a number of additional features, for instance the formation of gaps between the soil and pile, and by time effects due to consolidation, soil skeleton viscous behaviour, and so-called “set up” due to other, possibly unidentified, causes. We seek here just to define a basic rate-independent model.

The detailed description of the relevant equations and calibration of this model against a test database is the subject of Abadie, Houlsby and Byrne (2016), and (for a slightly different variant of the model) Abadie (2015). Here we just present the final result of the fitting.

We first fit the initial monotonic curve (establishing H_n and k_n , $n=0\dots N_S$), and then define the ratcheting behaviour, which may entail some minor adjustment of the parameters fitted to the initial loading curve, as well as establishing new parameters.

Monotonic loading

Ignoring ratcheting for the time being (*i.e.* $R_n = 0$), we fit the monotonic loading curve with a simple power-law curve, as shown in Figure 10. Such a relationship is found to fit observed pile loading data well, and is expressed as:

$$\varepsilon = \frac{\sigma}{E_0} + \varepsilon_{pU} \left(\frac{\sigma}{k_U} \right)^{m_h} \quad \dots(37)$$

where k_U , and ε_{pU} are appropriate normalizing quantities for stress and strain, m_h is an exponent and E_0 the initial stiffness. We first fix E_0 as a constant and choose k_U to be larger than any stress to be modelled subsequently. The relationship in (37) may be fitted to data either by eye or using least-squares curve fitting to select the two remaining monotonic loading parameters, ε_{pU} and m_h . The value of the exponent m_h may conveniently be estimated from the strain intercept at $k_U/2$, when the plastic strain is $\varepsilon_{pU}/2^{m_h}$.

We then choose k_n to represent a series of N_S equally spaced yield surfaces varying in size up to the limit k_U , in the form $k_n = k_U \frac{n}{N_S}$. The power law curve (for stresses not exceeding k_U) is then achieved by setting $H_0 = E_0$ and:

$$H_n = \frac{k_U}{N_S \varepsilon_{pU}} \times \frac{N_S^{m_h}}{(n+1)^{m_h} - 2n^{m_h} + (n-1)^{m_h}}, \quad 1 \leq n \leq N_S \quad \dots(38)$$

Ratcheting

For this particular model we choose the evolution law for the hardening parameter to be $\dot{\beta} = |\dot{\alpha}_r|$, in other words the hardening parameter β is the accumulated plastic strain.

To accommodate ratcheting behaviour we fix H_n , $0 \leq n \leq N_s$ to be constants, noting that if instead they were functions of state (through ε , α_n , α_r or β), then the appropriate derivatives of f would involve additional terms. In contrast, the values of k_n and R_n may be functions of state (specifically through σ and β) without affecting the differentials of d .

In order to accommodate the change in shape of the hysteresis loop during ratcheting, the strengths must be a function of the hardening variable, and this can be achieved by modifying the strengths to:

$$k_n = \left(k_U \frac{n}{N_s} \right) \left(\frac{\beta}{\beta_o} \right)^{m_k} \quad \dots(39)$$

where β_o is the initial value of β , and m_k is an exponent.

The most subtle of the quantities to fit are the ratcheting parameters R_n . We wish to achieve the following properties:

- $\dot{\alpha}_r$ should increase in a non-linear fashion with the magnitude of stress (higher stresses cause markedly more ratcheting),
- $\dot{\alpha}_r$ should reduce as β increases (modelling the reduction in rate of accumulation of ratcheting strain).

Satisfying these criteria, we choose:

$$R_n = R_o \left(\frac{k_n}{k_U} \right) \left(\frac{\beta}{\beta_o} \right)^{-m_r} \left(\frac{|\sigma|}{k_U} \right)^{m_s} \quad \dots(40)$$

with, for simplicity, the same value of ratcheting parameter for all yield surfaces. Note that in equation 40 the value of σ is the current stress and not the magnitude of a stress cycle, so the model is able to accommodate any pseudo-random load sequence as well as regular cycling.

The arbitrary choice has been made to fit all the relevant functions as power expressions: different forms could be chosen if they were justified by appropriate experimental data. The complete set of parameters for the model is given in Table 1.

Figure 11(a) shows the results of 1000 cycles of loading from $\sigma = 0.08$ to $\sigma = 0.55$ with the parameters shown in Table 1. Cycles 1, 10, 100 and 1000 are highlighted.

Figure 11(b) shows the results of an accelerated analysis, equivalent to that illustrated in Figure 11, but using just 50 cycles to simulate the same history, using the factors detailed in Table 2. Cycles 1, 10, 30 (equivalent to 100) and 50 (equivalent to 1000) are highlighted. The specific example used here involves $m_k = 0$, so that the strength parameters are constant, with the consequence that the acceleration procedure is exact in this case. At the end of the analysis not only is the accumulated displacement very close in the two analyses, but the shape of the final hysteresis loops is also matched. The small difference in accumulated displacement is entirely attributable to the numerical implementation of the model.

We have described a “macro model” which encapsulates the entire pile response within a single relationship between H and u . Whilst this is often an efficient way representing foundation behaviour within a structural analysis, for other applications it is of course necessary to address the distributed loads along the pile in more detail. As the observed macroscopic response simply reflects the integration of a more detailed pile-soil interaction, we suggest that the same principles as embodied in HARM may be applied to what is known in the industry as a “ p - y ” model of pile response, that is to say a model in which the lateral soil reaction at any point along the pile is solely a function of the history of deflection at that point (also called a generalised Winkler method). Beuckelaers (2015) presented a model where the Masing rules are applied to the “ p - y ” curves, and the development of the HARM model for application to the “ p - y ” method is pursued further by Beuckelaers *et al.* (2016).

Taking this one step further, we expect our macroscopic model to reflect the constitutive behaviour of the soil at a microscopic level, so that the constitutive model for the soil itself should embody the same principles as the HARM model. The suggested form of a tensorial model in Section 8 could for instance serve as the starting point for the modelling of undrained clay behaviour.

10. Conclusions

We have presented here one-dimensional models that are capable of modelling ratcheting phenomena. The models are extensions of multiple-surface plasticity models, using either the series or parallel configuration of spring-slider units. An additional “ratcheting strain” is introduced through the use of constraints. The realistic phenomena of reduced ratcheting rate, increased secant stiffness and reduced hysteresis with increasing cycle number can all be accommodated. Because they can be expressed in fully incremental form, the models are readily incorporated into numerical codes and are capable of making predictions for any stress path, without recourse to empirical rules depending on cycle counting. An acceleration procedure for mimicking the effects of very large numbers of cycles by analysis of a reduced number of cycles is described, employing a simple factor that accelerates the ratcheting effect. The models are readily extended to two dimensions, and to full tensorial forms to model material behaviour.

Acknowledgements

The second author was supported during the early development of this work by EDF Energies Nouvelles and EDF R&D. The third author is supported by the PISA project (funded by the Carbon

Trust through the Offshore Wind Accelerator, involving DONG Energy, Alstom, EDF Energies Nouvelles, Iberdrola, RWE, SSE, Statoil, Statkraft, Vattenfall and Van Oord).

References

- Abadie, C.N. (2015)** Cyclic lateral loading of monopile foundations in cohesionless soils, D.Phil. Thesis, University of Oxford
- Abadie, C.N., Byrne, B.W. and Houlsby, G. T. (2016)** Cyclic plastic response of large diameter monopiles in sand, Submitted to *Géotechnique*
- Armstrong, P.J. and Frederick, C.O. (1966)** A mathematical representation of the multiaxial Bauschinger effect, CEGB Report RD/B/N731, Berkeley Nuclear Laboratories, Berkeley, UK
- Bari, S. and Hassan, T. (2000)** Anatomy of coupled constitutive models for ratcheting simulation, *Int. Jour. of Plasticity*, 16(3), pp 381-409
- Beuckelaers, W.J.A.P. (2015)** Fatigue life calculation of monopiles for offshore wind turbines using a kinematic hardening soil model, *Proc. 24th European Young Geotechnical Engineering Conference (EYGEC)*, Durham, UK
- Beuckelaers, W.J.A.P., McAdam, R.A., Burd, H.J. Houlsby, G.T. and Byrne, B.W. (2016)** A generalised Winkler model for the hysteretic and ratcheting behaviour of monopiles in clay and sand, In preparation for submission to *Géotechnique*
- Chaboche, J.-L. (1986)** Time-independent constitutive theories for cyclic plasticity. *Int. Jour. of Plasticity* 2(2), pp 149-188.
- Chaboche, J.-L. (1991)** On some modifications of kinematic hardening to improve the description of ratchetting effects. *Int. Jour. of Plasticity* 7(7), pp 661-678.
- Chaboche, J.-L. and Nouailhas, D. (1989)** Constitutive modeling of ratchetting effects. Part II. Possibilities of some additional kinematic rules. *Jour. of Engineering Materials and Technology, Transactions of the ASME*, 111(4), pp 409-416.
- Collins, I.F. and Houlsby, G.T. (1997)** Application of Thermomechanical Principles to the Modelling of Geotechnical Materials, *Proc. of the Royal Society of London, Series A*, 453, pp 1975-2001 [doi:10.1098/rspa.1997.0107](https://doi.org/10.1098/rspa.1997.0107)
- Dettmer, W. and Reese S. (2004)** On the theoretical and numerical modelling of Armstrong-Frederick kinematic hardening in the finite strain regime, *Computer Methods in Applied Mechanics and Engineering*, 193, pp 87-116
- Germain, P., Nguyen, Q.S. and Suquet, P. (1983)** Continuum thermodynamics, *Trans. ASME, Jour. of Applied Mechanics*, 50(4B), pp 1010-1020
- Gerolymos, N., Papakyriakopoulos, O., Brinkgreve, R.B.J. (2014)** Macroelement modeling of piles in cohesive soil subjected to combined lateral and axial loading. *Proc. 8th Eur. Conf. on Numerical Methods in Geotechnical Engineering*, Delft, 18–20 June, Balkema, Rotterdam
- Houlsby, G.T. (1981)** A study of plasticity theories and their applicability to soils, Ph.D. Thesis, University of Cambridge www.repository.cam.ac.uk/handle/1810/250783
- Houlsby, G.T. and Cassidy, M.J. (2002)** A plasticity model for the behaviour of footings on sand under combined loading, *Géotechnique*, 52(2), pp 117-129 [doi:10.1680/geot.52.2.117.40922](https://doi.org/10.1680/geot.52.2.117.40922)
- Houlsby, G.T. and Puzrin, A.M. (2000)** A thermomechanical framework for constitutive models for rate-independent dissipative materials, *Int. Jour. of Plasticity*, 16(9), pp 1017-1047 [doi:10.1016/S0749-6419\(99\)00073-X](https://doi.org/10.1016/S0749-6419(99)00073-X)
- Houlsby, G.T. and Puzrin, A.M. (2002)** Rate-dependent plasticity models derived from potential functions, *Jour. of Rheology*, 46(1), pp 113-126 [doi:10.1122/1.1427911](https://doi.org/10.1122/1.1427911)

- Houlsby, G.T. and Puzrin, A.M. (2006)** *Principles of Hyperplasticity: an Approach to Plasticity Theory Based on Thermodynamic Principles*, Springer Verlag, London, 375 pp
- Lemaitre, J. and Chaboche, J.-L. (2010)** *Mécanique des matériaux solides*, 3rd edition, DUNOD, Paris
- LeBlanc, C., Houlsby, G.T. and Byrne, B.W. (2010)** Response of Stiff Piles in Sand to Long-term Cyclic Lateral Loading, *Géotechnique*, 60(2), pp 79-90 [doi:10.1680/geot.7.00196](https://doi.org/10.1680/geot.7.00196)
- LeBlanc, C., Byrne, B.W. and Houlsby, G.T. (2010)** Response of Stiff Piles to Random Two-Way Lateral Loading, *Géotechnique*, 60(9), pp 715-721 [doi:10.1680/geot.09.T.011](https://doi.org/10.1680/geot.09.T.011)
- Martin, C.M. and Houlsby, G.T. (2001)** Combined loading of spudcan foundations on clay: numerical modelling, *Géotechnique*, 51(8), pp 687-700 [doi:10.1680/geot.51.8.687.40470](https://doi.org/10.1680/geot.51.8.687.40470)
- Masing, G. (1926)** Eigenspannungen und verfestigung beim messing (Self stretching and hardening for brass), *Proc. 2nd Int. Congress for Applied Mechanics*, Zurich, Switzerland, pp 332–335 (in German)
- Moreau, J.J. (1970)** Sur les lois de frottement, de viscosité et de plasticité, *Comptes Rendus Acad. Sci.*, Paris, 271, pp 608-611 (in French)
- Nova, R. and Montrasio, L. (1991)** Settlements of shallow foundations on sand, *Géotechnique*, 41(2), pp 243-256
- Ohno, N. and Wang, J. (1995)** On modelling of kinematic hardening for ratcheting behaviour. *Nuclear Engineering and Design*, 153(2-3), pp 205-212
- Puzrin, A.M. and Houlsby, G.T. (2001a)** A thermomechanical framework for rate-independent dissipative materials with internal functions, *Int. Jour. of Plasticity*, 17, pp 1147-1165 [doi:10.1016/S0749-6419\(00\)00083-8](https://doi.org/10.1016/S0749-6419(00)00083-8)
- Puzrin, A.M. and Houlsby, G.T. (2001b)** Fundamentals of kinematic hardening hyperplasticity, *Int. Jour. of Solids and Structures*, 38(21), pp 3771-3794 [doi:10.1016/S0020-7683\(00\)00238-9](https://doi.org/10.1016/S0020-7683(00)00238-9)
- Schotman, G.J.M. (1989)** The effects of displacements on the stability of jack-up spudcan foundations, *Proc. 21st Offshore Technology Conference*, Houston, paper OTC 6026
- Suquet, P. (1982)** Plasticité et homogénéisation, Thesis, Université Pierre et Marie Curie, Paris
- Ziegler, H. (1963)** Some extremum principles in irreversible thermodynamics with application to continuum mechanics, *Progress in Solid Mechanics*, 4, pp 93-193
- Ziegler, H. (1977)** (2nd Edition: 1983) *An Introduction to Thermomechanics*, North Holland, Amsterdam

Notation

d	Dissipation function
D	Pile diameter
E	Elastic stiffness
f	Helmholtz free energy
g	Gibbs free energy
h	Height of load application point above ground surface
H	Applied load to pile
H_n	Stiffness parameter
k_n	Strength parameter
k_U	Upper value of k_n
L	Pile embedded length
m_h, m_k, m_r, m_s	Exponents used in power functions
n	Yield surface index, $1 \leq n \leq N_S$
N	Number of cycles
N_S	Number of yield surfaces
R_n	Ratcheting parameter (initial value at reference stress R_o)
R_{fac}	Factor on ratcheting parameter for accelerated modelling
u	Pile displacement at load application point
w	Flow potential
y	Yield surface, canonical form \bar{y}
z	Force potential
α	Internal variable (<i>e.g.</i> plastic strain)
α_n	Plastic strain component
α_r	Ratcheting strain
β	Hardening parameter (initial value β_o)

ε Strain

ε_{pU} Plastic strain at $\sigma = k_U$

μ Viscosity

σ Stress

$\chi_x, \bar{\chi}_x$ Generalised force conjugate to internal variable α_x

Special functions:

Macaulay bracket: $\langle x \rangle = \begin{cases} 0, & x \leq 0 \\ x, & x > 0 \end{cases}$

Modified signum function: $S(x) \in \begin{cases} \{-1\}, & x < 0 \\ [-1; +1], & x = 0 \\ \{+1\}, & x > 0 \end{cases}$, alternatively $S(x) = \begin{cases} a |a^2 \leq 1, & x^2 = 0 \\ \frac{x}{|x|}, & x^2 > 0 \end{cases}$

Vectorial signum function: $S_i(x) = \begin{cases} a_i |a_k a_k \leq 1, & x_k x_k = 0 \\ \frac{x_i}{\sqrt{x_k x_k}}, & x_k x_k > 0 \end{cases}$ (summation over the index k)

Tensorial signum function: $S_{ij}(x) = \begin{cases} a_{ij} |a_{kl} a_{kl} \leq 1, & x_{kl} x_{kl} = 0 \\ \frac{x_{ij}}{\sqrt{x_{kl} x_{kl}}}, & x_{kl} x_{kl} > 0 \end{cases}$ (summation over the indices k, l)

Appendix A: The hyperplastic formulation

A1: Basic formulation

Hyperplasticity (Houlsby and Puzrin, 2006) is an approach to plasticity theory, based on thermodynamic principles, in which the entire material response is derived from knowledge of two potential functions. The following is a brief summary of the key elements of the theory. Consider a system in which the mechanical behaviour is expressed in terms of strain ε and stress σ . The “state” of the material is also assumed to depend on “internal variables” α , which often (but not necessarily) play the role of plastic strain. In the following we are deliberately unspecific about the detailed nature of the internal variables. They can be in principle scalars, tensors, or multiple sets of tensors. In the case that the internal variables become an internal function (in effect an infinite number of variables), the potential functions become functionals, and the derivatives must be interpreted as Frechet derivatives (see Puzrin and Houlsby (2001) for details).

The formulation begins with the specification of a Helmholtz free energy $f(\varepsilon, \alpha)$, and a dissipation function $d(\varepsilon, \alpha, \dot{\alpha}) \geq 0$, which must be a homogeneous first order function of $\dot{\alpha}$ for a rate-independent (“plastic”) material, *i.e.* $d(\varepsilon, \alpha, \mu\dot{\alpha}) = \mu d(\varepsilon, \alpha, \dot{\alpha})$. The formulation then defines: $\sigma = \frac{\partial f}{\partial \varepsilon}$, $\bar{\chi} = -\frac{\partial f}{\partial \alpha}$ and $\chi = \frac{\partial d}{\partial \dot{\alpha}}$, where $\bar{\chi}$ and χ are “generalized stresses” conjugate to the internal variables α . It can be shown from thermodynamics that $(\bar{\chi} - \chi)\dot{\alpha} = 0$. If, however, we make the stronger assumption $\bar{\chi} = \chi$ (equivalent to the orthogonality postulate of Ziegler, 1977), then it follows that the entire constitutive response can now be derived without any further assumptions being necessary.

A2: Alternative forms

The formulation allows a variety of different potentials to be defined, and these are related by Legendre Transforms (or more generally Fenchel Duals). For instance, rather than specifying the Helmholtz free energy $f(\varepsilon, \alpha)$, it is possible to define the Gibbs free energy $g(\sigma, \alpha)$, defined by the Legendre transform $f + (-g) = \sigma\varepsilon$. In this case $\varepsilon = -\frac{\partial g}{\partial \sigma}$ and $\bar{\chi} = -\frac{\partial g}{\partial \alpha}$.

Instead of specifying the dissipation $d(\dots, \dot{\alpha})$, it is possible to specify the yield function in the form $y(\dots, \chi) = 0$. Here and in the following (...) stands for (ε, α) or (σ, α) , whichever is the most convenient form. The yield function may be written in a variety of ways, but we prefer the canonical form $\bar{y}(\dots, \chi) = \gamma(\dots, \chi) - 1$, where $\gamma(\dots, \chi)$ is the polar dual of $d(\dots, \dot{\alpha})$ defined by $\gamma(\dots, \chi) = \sup_{\dot{\alpha} \neq 0} \frac{\chi \dot{\alpha}}{d(\dots, \dot{\alpha})}$. The function $\gamma(\dots, \chi)$ is first order in χ , thus $\gamma(\dots, \mu\chi) = \mu\gamma(\dots, \chi)$. In this case

yield occurs when $\bar{y}(\dots, \chi) = 0$ and the plastic strain rates are determined by $\dot{\alpha} = \lambda \frac{\partial \bar{y}}{\partial \chi}$, where λ is a multiplier that becomes determined by the consistency condition $\bar{y} = 0$. The so-called Karush-Kuhn-Tucker (KKT) conditions apply: $\bar{y}\lambda = 0$ and $\bar{y} \leq 0, \lambda = 0$ or $\bar{y} = 0, \lambda \geq 0$.

A3: Rate dependence

It is often convenient for computation to introduce some rate-dependence (viscosity) into the analysis, and in this case rather than defining the dissipation function we can define either a force potential $z(...,\dot{\alpha})$, such that $\chi = \frac{\partial z}{\partial \dot{\alpha}}$ (instead of $\chi = \frac{\partial d}{\partial \dot{\alpha}}$), or a flow potential $w(...,\chi)$ such that $\dot{\alpha} = \frac{\partial w}{\partial \chi}$ (instead of $\dot{\alpha} = \lambda \frac{\partial \bar{y}}{\partial \chi}$). These are related by the Legendre transform $z + w = \chi \dot{\alpha} = d$. In the rate-independent case, where z is homogeneous and first order in $\dot{\alpha}$, then $z \equiv d$. See Houlsby and Puzrin (2002) for details.

A4: Constraints

The presence of a kinematic constraint $c(\dot{\alpha})=0$, the dissipation function is augmented by the use of a Lagrangian multiplier Λ times the constraint to form $d^*(...,\dot{\alpha})=d(...,\dot{\alpha})+\Lambda c(\dot{\alpha})$, and the generalized stress is given by $\chi = \frac{\partial d^*}{\partial \dot{\alpha}} = \frac{\partial d}{\partial \dot{\alpha}} + \Lambda \frac{\partial c}{\partial \dot{\alpha}}$. The multiplier Λ is then eliminated by using the constraint condition $c(\dot{\alpha})=0$.

A5: Passive kinematic variables

In certain applications it is convenient to exploit passive kinematic variables β (typically hardening parameters) which appear in the defining functions in the restricted form $f = f(\varepsilon, \alpha)$, $d = d(...,\beta, \dot{\alpha})$, $c = (c(\dot{\alpha}, \dot{\beta}))=0$. Application of the standard derivations yields $\sigma = \frac{\partial f}{\partial \varepsilon}$, $\bar{\chi} = -\frac{\partial f}{\partial \alpha}$, $\bar{\chi}_\beta = -\frac{\partial f}{\partial \beta} = 0$, $\chi = \frac{\partial d}{\partial \dot{\alpha}} + \Lambda \frac{\partial c}{\partial \dot{\alpha}}$ and $\chi_\beta = \frac{\partial d}{\partial \dot{\beta}} + \Lambda \frac{\partial c}{\partial \dot{\beta}} = \Lambda \frac{\partial c}{\partial \dot{\beta}}$. It follows that $\Lambda = 0$ and the formulation simply reduces to the original form $\sigma = \frac{\partial f}{\partial \varepsilon}$, $\bar{\chi} = -\frac{\partial f}{\partial \alpha}$, $\chi = \frac{\partial d}{\partial \dot{\alpha}}$ together with the constraint $c(\dot{\alpha}, \dot{\beta})=0$ which provides the evolution equation for β in $d = d(...,\beta, \dot{\alpha})$.

Appendix B: Alternative functions and derivations

B1: Series model

The Gibbs free energy is:

$$g = -\frac{\sigma^2}{2H_0} - \sigma \sum_{n=1}^{N_s} \alpha_n + \sum_{n=1}^{N_s} \frac{H_n}{2} \alpha_n^2 \quad \dots(B.1)$$

The yield functions in canonical form are:

$$\bar{y}_n = \frac{|\chi_n|}{k_n} - 1 = 0 \quad \dots(B.2)$$

A rate-dependent variant of this model is defined by:

$$z = \sum_{n=1}^{N_s} \left(k_n |\dot{\alpha}_n| + \frac{\mu}{2} \dot{\alpha}_n^2 \right) \quad \dots(B.3)$$

or

$$w = \frac{1}{2\mu} \sum_{n=1}^{N_s} \langle |\chi_n| - k_n \rangle^2 \quad \dots(B.4)$$

B2: Parallel model

The Gibbs free energy is:

$$g = -\frac{\left(\sigma + \sum_{n=1}^{N_s} H_n \alpha_n \right)^2}{2E_0} + \sum_{n=1}^{N_s} \frac{H_n}{2} \alpha_n^2 \quad \dots(B.5)$$

where $E_0 = \sum_{n=1}^{N_s+1} H_n$.

The canonical yield functions and the expressions for z and w are exactly as for the series model (equations B.2, B.3, B.4).

B3: s-HARM model

The Gibbs free energy is:

$$g = -\frac{\sigma^2}{2H_0} - \sigma \left(\sum_{n=1}^{N_s} \alpha_n + \alpha_r \right) + \sum_{n=1}^{N_s} \frac{H_n}{2} \alpha_n^2 \quad \dots(B.6)$$

Leading to:

$$\varepsilon = -\frac{\partial g}{\partial \sigma} = \frac{\sigma}{H_0} + \sum_{n=1}^{N_S} \alpha_n + \alpha_r \quad \dots(\text{B.7})$$

$$\bar{\chi}_n = -\frac{\partial g}{\partial \alpha_n} = \sigma - H_n \alpha_n, \quad n=1 \dots N_S \quad \dots(\text{B.8})$$

$$\bar{\chi}_r = -\frac{\partial f}{\partial \alpha_r} = \sigma \quad \dots(\text{B.9})$$

The yield functions (not in canonical form) are:

$$y_n = |\chi_n| - k_n + R_n (|\chi_r| - |\sigma|) = 0 \quad \dots(\text{B.10})$$

Leading to:

$$\dot{\alpha}_n = \lambda_n \frac{\partial y_n}{\partial \chi_n} = \lambda_n S(\chi_n) \quad \dots(\text{B.11})$$

$$\dot{\alpha}_r = \sum_{n=1}^{N_S} \lambda_n \frac{\partial y_n}{\partial \chi_r} = \sum_{n=1}^{N_S} \lambda_n R_n S(\chi_r) = S(\sigma) \sum_{n=1}^{N_S} R_n |\dot{\alpha}_n| \quad \dots(\text{B.12})$$

The rate-dependent version of the model can be determined by the force potential:

$$z = \sum_{n=1}^N \left(k_n |\dot{\alpha}_n| + \frac{\mu}{2} \dot{\alpha}_n^2 \right) + \sigma \dot{\alpha}_r \quad \dots(\text{B.13})$$

together with constraint

$$c_r = \dot{\alpha}_r - S(\sigma) \sum_{n=1}^{N_S} R_n |\dot{\alpha}_n| = 0 \quad \dots(\text{B.14})$$

Leading to use of the augmented force potential:

$$z^* = \sum_{n=1}^N \left(k_n |\dot{\alpha}_n| + \frac{\mu}{2} \dot{\alpha}_n^2 \right) + \sigma \dot{\alpha}_r + \Lambda_r \left(\dot{\alpha}_r - S(\sigma) \sum_{n=1}^{N_S} R_n |\dot{\alpha}_n| \right) \quad \dots(\text{B.15})$$

and:

$$\chi_n = \frac{\partial z^*}{\partial \dot{\alpha}_n} = k_n S(\dot{\alpha}_n) + \mu \dot{\alpha}_n - \Lambda_r S(\sigma) R_n S(\dot{\alpha}_n), \quad n=1 \dots N_S \quad \dots(\text{B.16})$$

$$\chi_r = \frac{\partial z^*}{\partial \dot{\alpha}_r} = \sigma + \Lambda_r \quad \dots(\text{B.17})$$

From which we obtain $\Lambda_r = 0$, so that:

$$\sigma - H_n \alpha_n = k_n S(\dot{\alpha}_n) + \mu \dot{\alpha}_n, \quad n=1 \dots N_S \quad \dots(\text{B.18})$$

or

$$\sigma - H_n \alpha_n = (k_n + \mu |\dot{\alpha}_n|) S(\dot{\alpha}_n) \quad \dots(\text{B.19})$$

Noting that the only solution for $|\sigma - H_n \alpha_n| < k_n$ is $\dot{\alpha}_n = 0$, and that $S(\sigma - H_n \alpha_n) = S(\dot{\alpha}_n)$ we can write this as:

$$\dot{\alpha}_n = \frac{1}{\mu} \langle |\sigma - H_n \alpha_n| - k_n \rangle S(\sigma - H_n \alpha_n), \quad n=1 \dots N_S \quad \dots(\text{B.20})$$

Alternatively the model can be derived from the flow potential:

$$w = \frac{1}{2\mu} \sum_{n=1}^{N_S} \langle |\chi_n| - k_n + R_n (|\chi_r| - |\sigma|) \rangle^2 \quad \dots(\text{B.21})$$

leading to

$$\dot{\alpha}_n = \frac{\partial w}{\partial \chi_n} = \frac{1}{\mu} \langle |\chi_n| - k_n + R_n (|\chi_r| - |\sigma|) \rangle S(\chi_n), \quad n=1 \dots N_S \quad \dots(\text{B.22})$$

$$\dot{\alpha}_r = \frac{\partial w}{\partial \chi_r} = \frac{1}{\mu} \sum_{n=1}^{N_S} \langle |\chi_n| - k_n + R_n (|\chi_r| - |\sigma|) \rangle R_n S(\chi_r) = S(\sigma) \sum_{n=1}^{N_S} R_n |\dot{\alpha}_n| \quad \dots(\text{B.23})$$

which in turn leads to:

$$\dot{\sigma} = H_0 \left(\dot{\varepsilon} - \sum_{n=1}^{N_S} \dot{\alpha}_n - \dot{\alpha}_r \right) = H_0 \left(\dot{\varepsilon} - \frac{1}{\mu} \sum_{n=1}^{N_S} \langle |\chi_n| - k_n + R_n (|\chi_r| - |\sigma|) \rangle (S(\chi_n) + R_n S(\chi_r)) \right) \quad \dots(\text{B.24})$$

or, for a small increment (and substituting some derived results):

$$d\sigma = H_0 d\varepsilon - \frac{H_0 dt}{\mu} \sum_{n=1}^N \langle |\sigma - H_n \alpha_n| - k_n \rangle (S(\sigma - H_n \alpha_n) + R_n S(\sigma)) \quad \dots(\text{B.25})$$

This latter form is particularly useful as, given the current state (in terms of σ and α_n) and a strain increment $d\varepsilon$ (or stress increment $d\sigma$) in a small time interval dt , it is possible to solve directly for the stress increment $d\sigma$ (or strain increment $d\varepsilon$). In order to complete the solution it is also necessary to update the internal variables. The complete set of incremental updating equations can be succinctly expressed by:

$$d\alpha_n = \frac{dt}{\mu} \langle |\sigma - H_n \alpha_n| - k_n \rangle S(\sigma - H_n \alpha_n), \quad n=1 \dots N_S \quad \dots(\text{B.26})$$

$$d\alpha_r = S(\sigma) \sum_{n=1}^{N_s} R_n |d\alpha_n| \quad \dots(B.27)$$

$$d\sigma = H_0 \left(d\varepsilon - \sum_{n=1}^{N_s} d\alpha_n - d\alpha_r \right) \quad \dots(B.28)$$

The two-dimensional model is most conveniently derived from the flow potential:

$$w = \frac{1}{2\mu} \sum_{n=1}^{N_s} \left\langle \sqrt{\chi_{1n}^2 + \chi_{2n}^2} - k_n + R_n \left(\sqrt{\chi_{1r}^2 + \chi_{2r}^2} - \sqrt{\sigma_1^2 + \sigma_2^2} \right) \right\rangle^2 \quad \dots(B.29)$$

B4: p-HARM model

The Gibbs free energy is:

$$g = - \frac{\left(\sigma + \sum_{n=1}^{N_s} H_n \alpha_n \right)^2}{2E_0} - \sigma \alpha_r + \sum_{n=1}^{N_s} \frac{H_n}{2} \alpha_n^2 \quad \dots(B.30)$$

Leading to:

$$\varepsilon = - \frac{\partial g}{\partial \sigma} = \frac{\sigma + \sum_{n=1}^{N_s} H_n \alpha_n}{E_0} + \alpha_r \quad \dots(B.31)$$

$$\bar{\chi}_n = - \frac{\partial g}{\partial \alpha_n} = H_n \frac{\sigma + \sum_{n=1}^{N_s} H_n \alpha_n}{E_0} - H_n \alpha_n = H_n (\varepsilon - \alpha_n - \alpha_r), \quad n=1 \dots N_s \quad \dots(B.32)$$

$$\bar{\chi}_r = - \frac{\partial f}{\partial \alpha_r} = \sigma \quad \dots(B.33)$$

Other results follow very closely the development of the s-HARM model.

Appendix C: The Armstrong-Frederick model in hyperplasticity terminology

The (one dimensional) Armstrong-Frederick model is represented diagrammatically in Figure 12 and can be derived from the following functions:

$$f = \frac{H_0}{2}(\varepsilon - \alpha_1)^2 + \frac{H_1}{2}(\alpha_1 - \alpha_{r1})^2 \quad \dots(\text{C.1})$$

$$d = k_1|\dot{\alpha}_1| + \bar{\chi}_{r1}\dot{\alpha}_{r1} \quad \dots(\text{C.2})$$

$$c = \dot{\alpha}_{r1} - \frac{\bar{\chi}_{r1}}{\chi^*}|\dot{\alpha}_1| = 0 \quad \dots(\text{C.3})$$

where H_0, H_1 are constants and k_1, χ^* are either constants or may be functions of state. Note that the constraint means that the second term in the dissipation is always assured as non-negative. We make use of the augmented dissipation function:

$$d^* = d + \Lambda c = k_1|\dot{\alpha}_1| + \bar{\chi}_{r1}\dot{\alpha}_{r1} + \Lambda \left(\dot{\alpha}_{r1} - \frac{\bar{\chi}_{r1}}{\chi^*}|\dot{\alpha}_1| \right) \quad \dots(\text{C.4})$$

and obtain the following derivatives:

$$\sigma = \frac{\partial f}{\partial \varepsilon} = H_0(\varepsilon - \alpha_1) \quad \dots(\text{C.5})$$

$$\bar{\chi}_1 = -\frac{\partial f}{\partial \alpha_1} = H_0(\varepsilon - \alpha_1) - H_1(\alpha_1 - \alpha_{r1}) = \sigma - \bar{\chi}_{r1} \quad \dots(\text{C.6})$$

$$\bar{\chi}_{r1} = -\frac{\partial f}{\partial \alpha_{r1}} = H_1(\alpha_1 - \alpha_{r1}) \quad \dots(\text{C.7})$$

$$\chi_1 = \frac{\partial d^*}{\partial \dot{\alpha}_1} = k_1 S(\dot{\alpha}_1) - \Lambda \frac{\bar{\chi}_{r1}}{\chi^*} S(\dot{\alpha}_1) \quad \dots(\text{C.8})$$

$$\chi_{r1} = \frac{\partial d^*}{\partial \dot{\alpha}_{r1}} = \bar{\chi}_{r1} + \Lambda \quad \dots(\text{C.9})$$

It immediately follows that $\Lambda = 0$ and that the yield surface in stress space is determined by:

$$|\sigma - \bar{\chi}_{r1}| = k_1 \quad \dots(\text{C.10})$$

So that $\bar{\chi}_{r1}$ plays the role of a back-stress. In the diagrammatic form, Figure 12, the back stress can be identified with the force in the spring element H_1 .

Making use of the incremental relationship:

$$\dot{\bar{\chi}}_{r1} = H_1(\dot{\alpha}_1 - \dot{\alpha}_{r1}) \quad \dots(\text{C.11})$$

and combining this with the constraint, one can obtain:

$$\dot{\bar{\chi}}_{r1} = H_1 \left(\dot{\alpha}_1 - \frac{\bar{\chi}_{r1}}{\chi^*} |\dot{\alpha}_1| \right) \quad \dots(\text{C.12})$$

which can be identified as the Armstrong-Frederick form of the evolution law for the back-stress $\bar{\chi}_{r1}$.

Note that Dettmer and Reese (2004) explain the AF model using a very similar diagram to Figure 12, but instead of the ratcheting element they employ a dashpot with a “pseudo-viscosity” that is inversely proportional to the strain rate magnitude in the main sliding element $|\dot{\alpha}_1|$. Noting that the

constraint implies that $\bar{\chi}_{r1} = \chi^* \frac{\dot{\alpha}_{r1}}{|\dot{\alpha}_1|}$, our approach above could be described in a similar way, giving

$$d = k_1 |\dot{\alpha}_1| + \frac{\chi^*}{|\dot{\alpha}_1|} \dot{\alpha}_{r1}^2, \text{ where } \frac{\chi^*}{|\dot{\alpha}_1|} \text{ is identified as the “pseudo-viscosity”}.$$

Tables

	Constant	Value	Dimension
Monotonic loading parameters	E_0	85.0	stress/strain
	k_U	1.0	stress
	ε_{pU}	1.0	strain
	m_h	3.2	-
Ratcheting parameters	R_o	4000.0	-
	β_o	0.05	strain
	m_r	4.5	-
	m_s	5.0	-
	m_k	0.0	-
Modelling parameters	N_s	40	-
	μ	0.1	stress x time / strain
	δt	0.0033	time
Cycle period	T	10.0	time

Table 1: Model parameters used in simulations

Figure 11 (normal analysis)	Figure 12 (accelerated analysis)
10 cycles $R_{fac} = 1$	10 cycles $R_{fac} = 1$
80 cycles $R_{fac} = 1$	10 cycles $R_{fac} = 8$
10 cycles $R_{fac} = 1$	10 cycles $R_{fac} = 1$
890 cycles $R_{fac} = 1$	10 cycles $R_{fac} = 89$
10 cycles $R_{fac} = 1$	10 cycles $R_{fac} = 1$
Total analysis cycles: 1000 Total simulated cycles: 1000	Total analysis cycles: 50 Total simulated cycles: 1000

Table 2: Cyclic loading program for normal and accelerated analyses

Figures

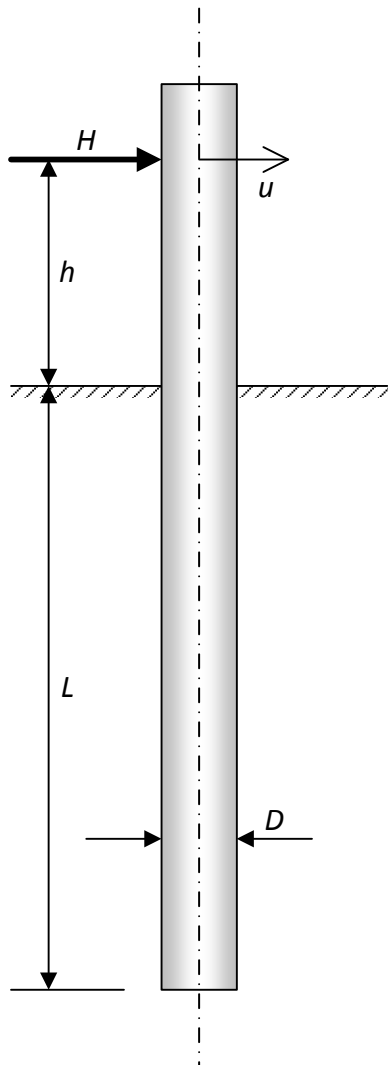


Figure 1: pile loading

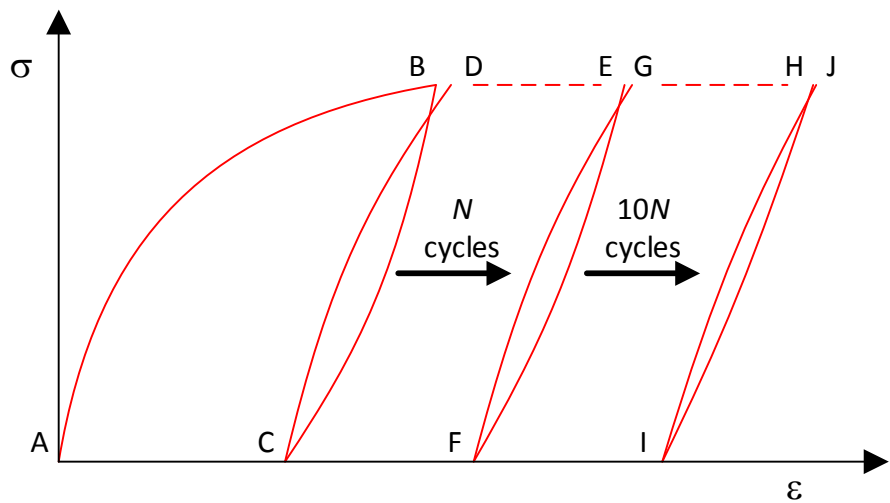


Figure 2: principle features of 1-D cyclic loading

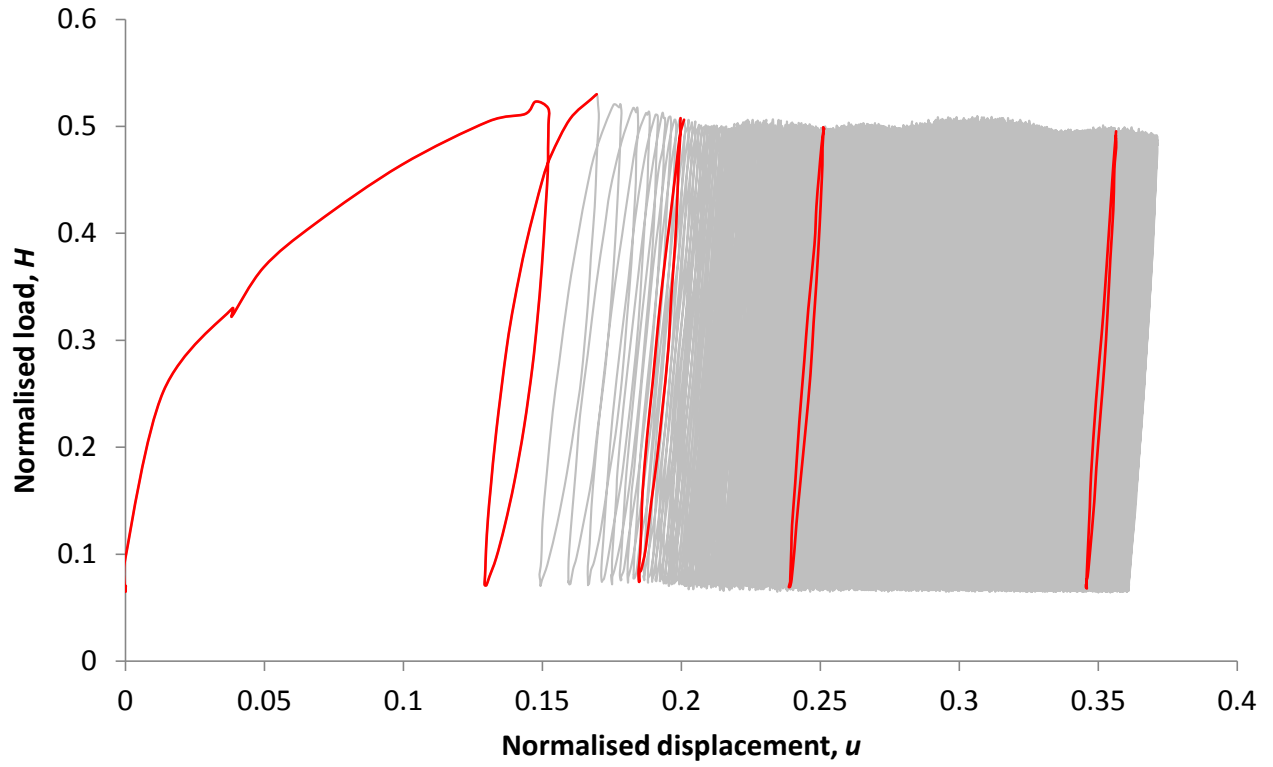


Figure 3: example pile loading test, Abadie (2015). First, 10th, 100th and 1000th cycles highlighted

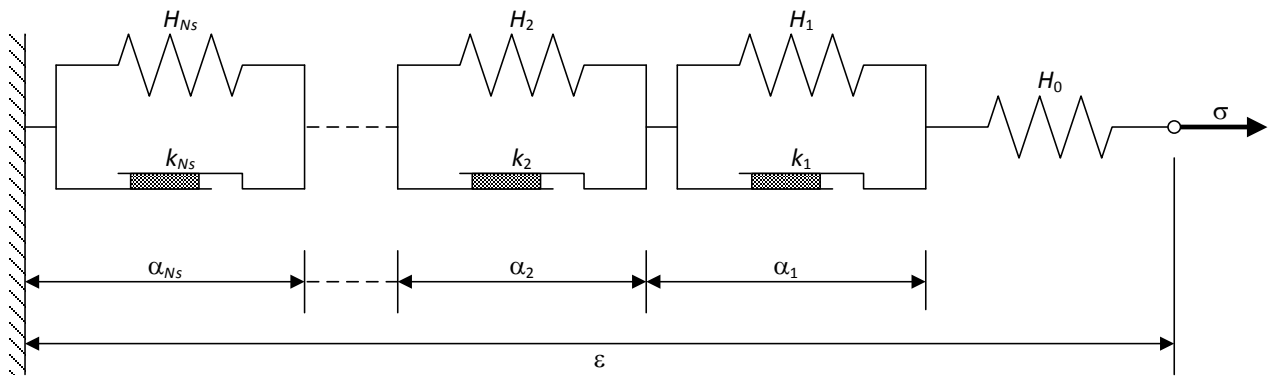


Figure 4: multiple surface kinematic hardening plasticity (series form)

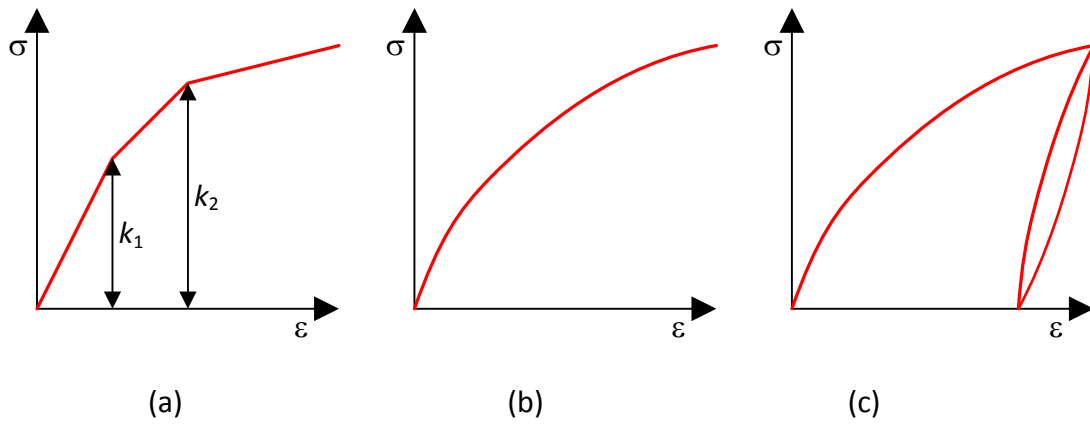


Figure 5: kinematic hardening plasticity: (a) multisurface model, (b) limit as $N_s \rightarrow \infty$, (c) hysteresis on unloading

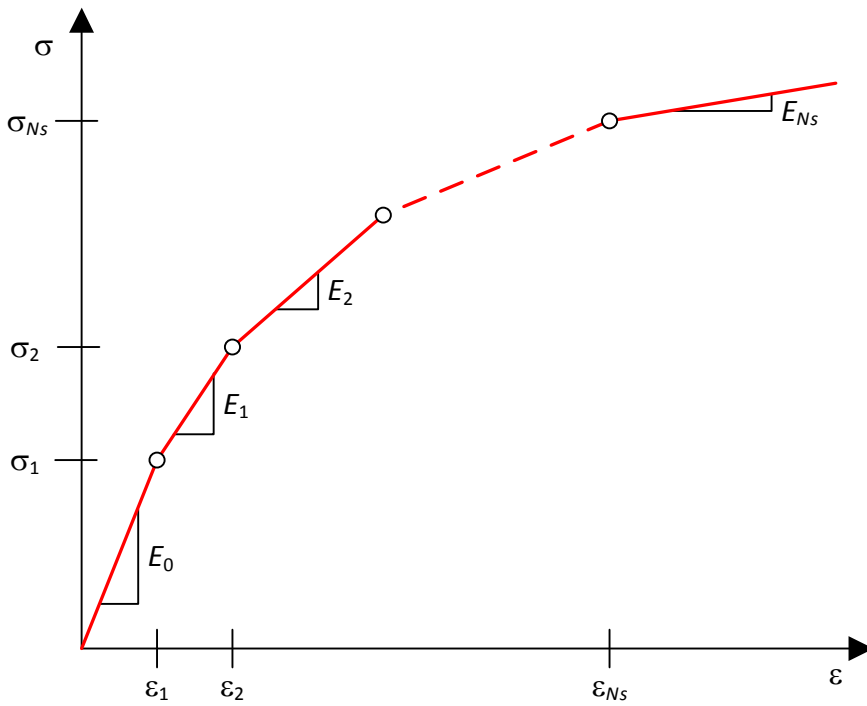


Figure 6: stress strain curve for multiple yield surface model

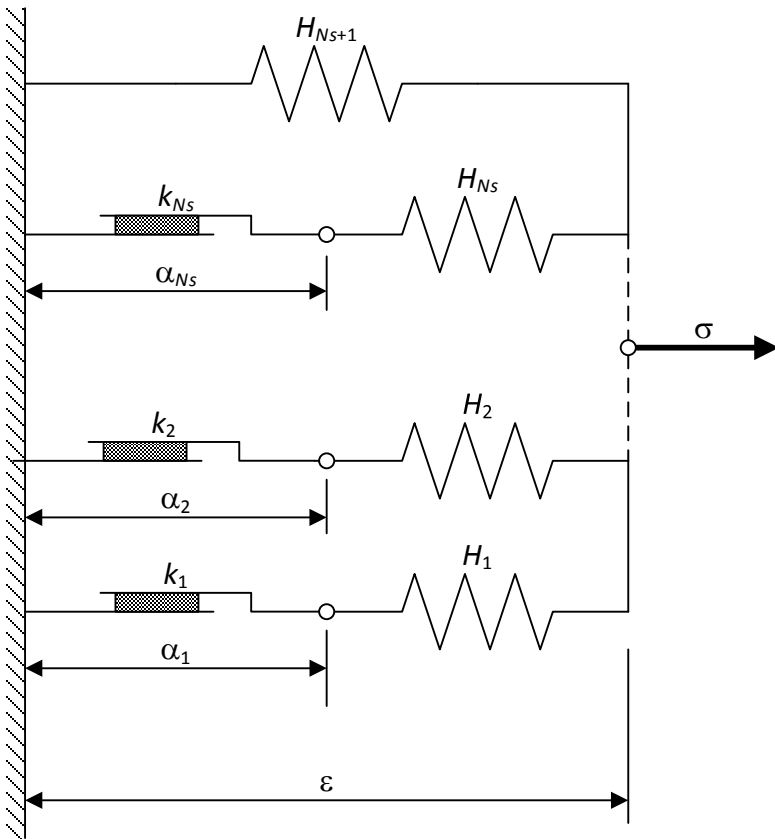


Figure 7: multiple surface kinematic hardening plasticity (parallel form)

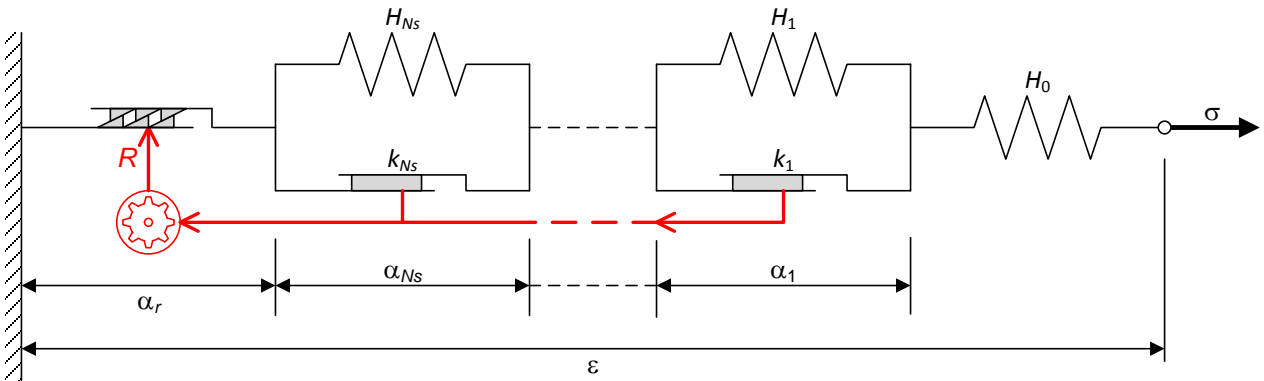
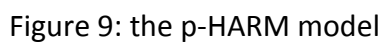


Figure 8: the s-HARM model



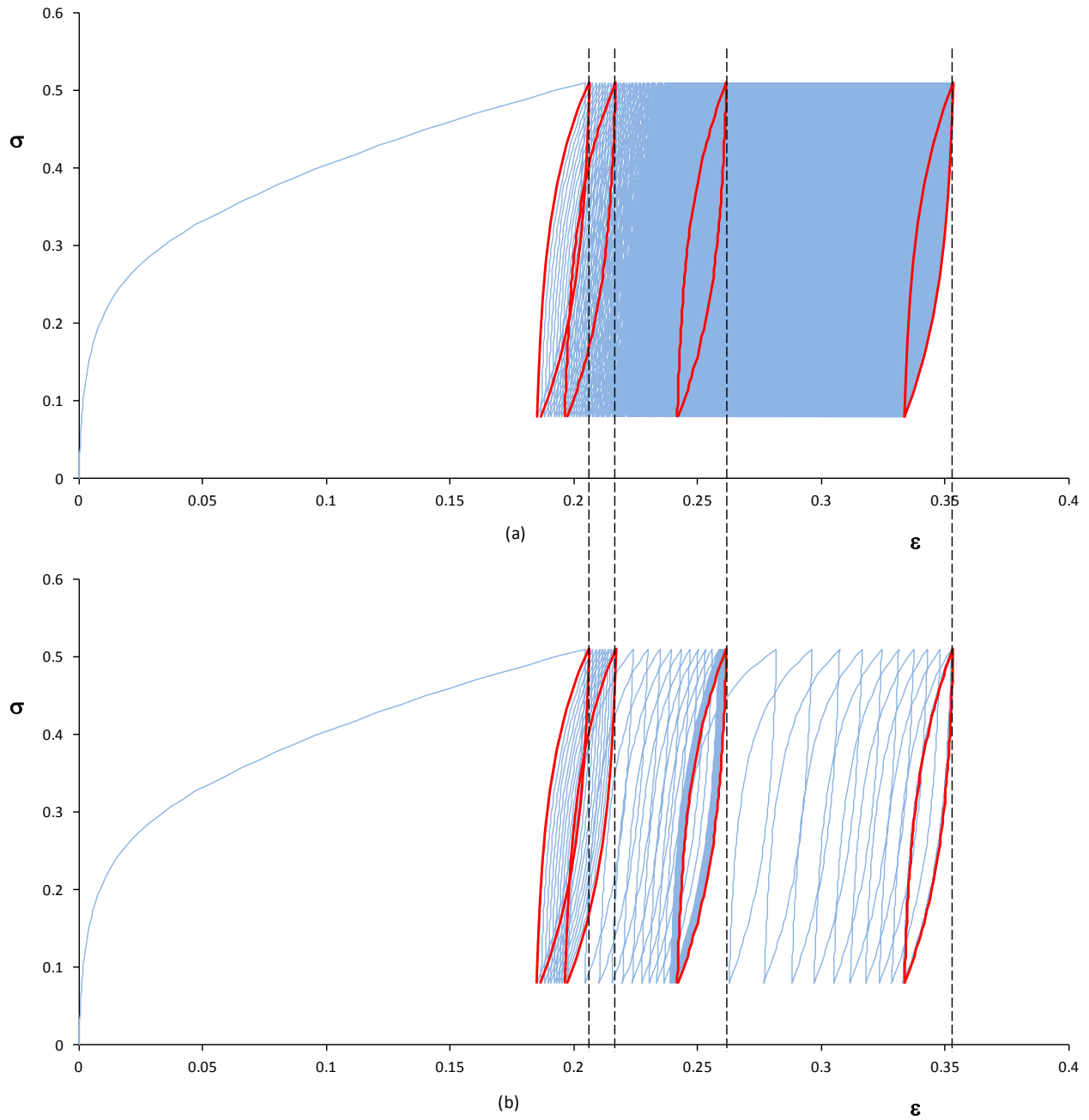


Figure 11: (a) 1000 cycles. Cycles 1, 10, 100 and 1000 highlighted, (b) 1000 cycles simulated by 50 cycles with adjusted rate parameter. Cycles 1, 10, 30 (equivalent to 100) and 50 (equivalent to 1000) highlighted

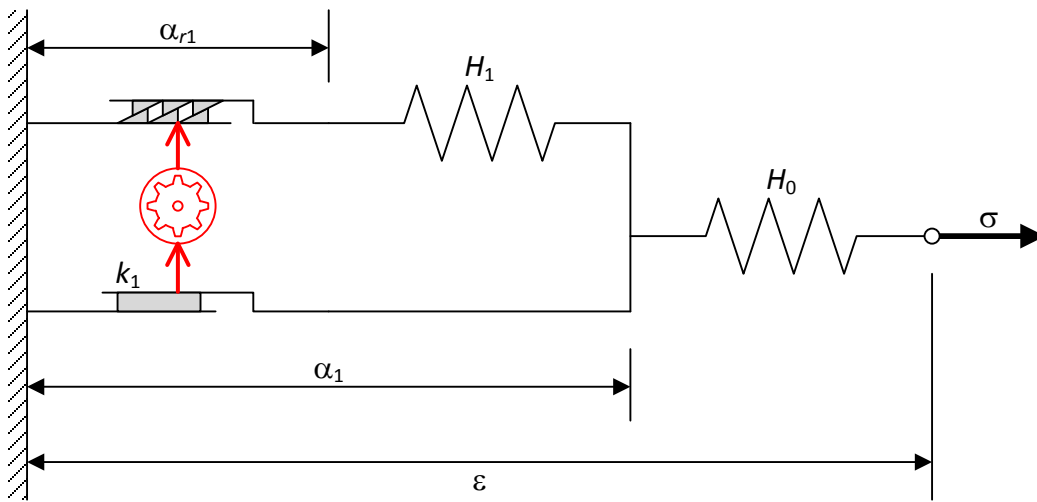


Figure 12: diagrammatic representation of the Armstrong-Frederick model